Results in Physics 39 (2022) 105753

Contents lists available at ScienceDirect

Results in Physics

journal homepage: www.elsevier.com/locate/rinp

Optical solitons and qualitative analysis of nonlinear Schrodinger equation in the presence of self steepening and self frequency shift

Farwa Salman [a], Nauman Raza [a], Ghada Ali Basendwah [b], Mohammed M.M. Jaradat [c,*]

[a] Department of Mathematics, University of the Punjab, Quaid-e-Azam Campus, Lahore, Pakistan
[b] Department of Mathematics, King Abdulaziz University, Jeddah, Saudi Arabia
[c] Mathematics Program, Department of Mathematics, Statistics and Physics, College of Arts and Sciences, Qatar University, Doha P.O. Box 2713, Qatar

ARTICLE INFO

Keywords:
Cubic quintic NLSE
Optical solitons
Polynomial and rational form solutions
Bifurcation

ABSTRACT

In this manuscript, the optical solitons of nonlinear Schrödinger equation (NLSE) with cubic–quintic law nonlinearity, in the presence of self-frequency shift and self-steepening, has been studied. The ultrahigh capacity propagation and transit of laser light pulses in optical fibres were described using this form of equation. To extract new results, two strong methodologies has been used. To extract the exact solution unified method has been employed. The solutions obtained by this analytical method, are in form of polynomial and rational function solution. Moreover, the validity of non-singular solutions has guaranteed by a limitation condition that is graphically illustrated in 3D. The 2D graphical representation are also used to demonstrate the influence of parameters on the predicted non-singular solutions. The other technique, used for qualitative analysis, is bifurcation. The system has been transformed into a planer dynamical system, which has been transformed into a hamiltonian system. All the possible phase portrait has been plotted by complete discrimination method. The acquired results are novel and have not been recorded before and they indicate that the proposed methodologies may be used to investigate innovative soliton solutions and phase portraits for any NLSE.

Introduction

Fiber optics is a popular discipline in the modern field of nonlinear optical communication study. It is crucial to upgrade optical fibre transmission systems in order to meet the demands of information transfer based technologies [1–3]. Soliton dynamics is a prominent topic of investigation in mathematics and physics that has wide range of applications, especially in fibre optics [4–8]. In 1834, John Scott Russell saw a solitary wave in the Union Canal in Scotland that was the first to report the soliton phenomenon. He reproduced the event in a wave tank and named it the“Wave of Translation" [9]. Soliton describes a pulse that looks like a nonlinear wave and develops after colliding with another pulse of comparable form and speed.

In nonlinear optics, NLSE was developed to enhance optical communication quality. Communication over fibre optics takes only a few femtoseconds. By concentrating on the most vital elements of NLSE, the soliton solution can be discovered. NLSE is essential in a variety of physical phenomena and scientific disciplines, including plasma physics, optical fibres, thermodynamics, fluid mechanics, wave propagation, chemical physics, biology, and so on [10–25]. There are variety of integration strategies for solving NLSE that can provide understanding of the real behavior of various systems. Famous analytical methodologies have been used to determine analytical answers to NLSE in recent years. These include the sine cosine method [26], the homogeneous balance method [27,28], the Riccati–Bernoulli sub-ODE method [29,30], the tanh method [31], the inverse scattering method [32], (G’/G)-expansion method [33,34], simple equation method [35,36], and the extended trial equation method [37,38].

The presented article deals with the NLSE with cubic–quintic law nonlinearity, in the presence of self-frequency shift and self-steepening, has been studied. The ultrahigh capacity propagation and transit of laser light pulses in optical fibres were described using this form of equation. This equation is of great interest for many mathematicians and physicists. Chirped chiral solitons for this equation has been extracted and the obtained solutions are periodic and localized solutions of dark–bright solitons [39]. The dark and bright solitary wave solutions has been achieved by applying solitary wave ansatz method [40]. This model has also been investigated to find the chirped femtosecond solitons and double-kink solitons in which the amplitude of the chirping can be controlled by self frequency shift and self-steepening [41]. In this paper new traveling wave solutions has been exhibit in form of

* Corresponding author.
E-mail address: mmjst4@qu.edu.qa (M.M.M. Jaradat).

https://doi.org/10.1016/j.rinp.2022.105753
Received 21 May 2022; Received in revised form 13 June 2022; Accepted 17 June 2022
Available online 25 June 2022

polynomial and rational form also qualitative analysis of this model has never been investigated by any author yet. Hence our acquired results are novel and will be a good addition in literature.

The aim of this article is using the unified method [42,43] to determine the exact solution related to governing model. The proposed technique is preferable on other techniques because the solutions can be extracted in form of polynomial and rational solutions. The solutions are recorded and shown graphically. The dynamical system of the noted equation's bifurcation is also discussed. All conceivable possibilities for parameter dependency are studied, using the bifurcation theory of planner dynamical systems [44–46], in order to show phase illustrations of the behavior of the governing differential equation.

The article is divided into 7 sections. The overview of the proposed techniques is given in Section 'Governing Model'. Section 'A concise overview of the unified approach' discussed the governing equation. The extraction of the exact solution of governing differential equation has been provided in Section 'Analytical soliton solutions'. Polynomial and rational function solutions are provided in Section 'Analytical soliton solutions'. Section 'Applications' discusses the graphical illustration of solutions of the governing equation. Bifurcation analysis with the dynamical planner system has been presented in Section 'Qualitative Analysis of governing equation'. The conclusion of the presented article has been recorded in Section 'Conclusion'.

Governing model

The wave dynamics in fiber optics are represented by the NLSE. The dimension-less form of NLSE is given by

$$ip_t + b_1 p_{xx} + b_2 Q(|p|^2)p = ib_4(|p|^2 p)_x + ib_5(|p|^2)p, \tag{1}$$

in aforementioned equation $p(x,t)$ represents the non-real valued ripple profile and t and x represents the time and space variable accordingly. Here the term $Q(p) = p + b_3 p^2$ is used for cubic–quintic nonlinearity, by substituting the value of $Q(p)$ in Eq. (1), the equation becomes

$$ip_t + b_1 p_{xx} + b_2 Q(|p|^2)p + b_3(|p|^4)p = ib_4(|p|^2 p)_x + ib_5(|p|^2)p, \tag{2}$$

where b_1, b_4 and b_5 are the coefficient of dispersion, self-steepening and self-frequency shift. b_2 and b_3 are the cubic and quintic nonlinear coefficients. The coefficients b_2 and b_3 could be positive or negative, depending on whether the connection is attractive or not. The following transformation is utilized to deal with Eq. (2)

$$p(x,t) = \upsilon(\zeta)e^{\iota\theta}, \tag{3}$$

where $\zeta = A(x - \nu t)$. The $\upsilon(\zeta)$ denotes the amplitude of the wave, also $\theta = -kx + \omega t + \phi$ defines the phase element, while k is frequency, ω represents the wave number of soliton and phase constant is shown by ϕ. The relations can be formed by substituting Eq. (3) into Eq. (2) and splitting the real and imaginary components. The essential condition for the presence of soliton are derived from the imaginary part that is

$$\nu = -2b_1 k. \tag{4}$$

The real part of the equation is used to find the solution of Eq. (2). The real part is as follow

$$-(\omega + b_1 l k^2)\upsilon + b_1 A^2 \upsilon'' + (b_2 - kb_4)\upsilon^3 + b_3 \upsilon^5 = 0, \tag{5}$$

here ω, and k are unknown parameters. Now, we find $n = 1/2$ by analyzing the homogeneous balance principle between the highest order derivative and non linear terms in Eq. (5). To acquire a closed form solution, we used another transformation as follows

$$\upsilon(\zeta) = W^{1/2}(\zeta), \tag{6}$$

and Eq. (5) reduced as following manner

$$-(\omega + b_1 k^2)W^2 + b_1 A^2\left(-\frac{1}{4}(W')^2 + \frac{1}{2}WW''\right) + (b_2 - kb_4)W^3 + b_3 W^4 = 0. \tag{7}$$

A concise overview of the unified approach

In the presented article, we will extract the solution with the help of one of the best techniques that is unified method. The advantage of this method on other methods, is the form of solutions obtained by this analytical technique. By applying this technique the solution can be retrieved in form of polynomial and rational functions.

Let the complete structure of generalized NLSE be as in the following fashion;

$$U(x, t, v_x, v_t, v_{xt}, v_{xx}, v_{tt} ..., v_{mxt}) = 0, \quad m \geq 0, \tag{8}$$

where U representing the polynomial involving the function $\upsilon = \upsilon(x,t)$ which is unknown. The essential formulation of the unified method is illustrated below:

Through employing the traveling wave transformation of the following pattern

$$v(x,t) = p(\zeta), \quad \zeta = kx + lt, \tag{9}$$

here k and l are arbitrary constants, Eq. (8) transformed to an ODE as follow

$$P(\zeta, \zeta', \zeta'', \dots, \zeta^m) = 0, \tag{10}$$

here P' shows the differentiation of P involving the new variable ζ. The unified method is used to explore the exact solution of Eq. (10), which allows to reveal the solution in form of polynomial and rational function solution. It has been discussed in more detail below.

⋆ Polynomial function solution

Consider that Eq. (10) has the polynomial solution as

$$P(\zeta) = \sum_{i=0}^{n} p_i \psi^i(\zeta). \quad p_i \neq 0. \tag{11}$$

In aforementioned equation, p_i's are constants and function $\psi(\zeta)$ is acquired by solving the auxiliary equation:

$$(\psi'(\zeta))^\gamma = \sum_{i=0}^{\rho k} r_i \psi^i(\zeta), \qquad \zeta = \mu z - \nu t, \quad \gamma = 1, 2, \tag{12}$$

here $r_i's$ are arbitrary parameters and the numeric value of n is defined in terms of k by inserting the homogeneous balance condition between highest derivative and the highest non-linear term in (2), while k can be determined using the consistency criteria.

Presently to solve Eq. (11), the unified method tackles Eq. (11) for elementary and elliptic solutions when $\gamma = 1$ or $\gamma = 2$ individually.

⋆ Rational function

Principle idea of stated part is to consider that (2) has the solution as

$$P(\zeta) = \frac{\sum_{m=0}^{n} a_m \psi^m(\zeta)}{\sum_{m=0}^{r} b_m \psi^m(\mu)}, \quad n \geq r, \tag{13}$$

with satisfying auxiliary equation,

$$(\psi'(\zeta))^\gamma = \sum_{i=0}^{ns} \beta_i \psi^i(\zeta), \qquad \zeta = kx + lt, \quad \gamma = 1, 2. \tag{14}$$

a_i, b_i, and β_i are the constants to be found in Eqs. (13) and (14), in such a way that the solution obtained by Eq. (13) fulfills Eq. (2).

The values of n and s could be found by using balancing principle between the highest order of linear and nonlinear terms included in Eq. (2). Likewise, we may determine the unknown coefficients in Eq. (13) by using condition of consistency. The unified method will apply to solve the Eq. (13). Then we get solutions for $\gamma = 1$ or $\gamma = 2$, accordingly.

$$W(\zeta)=\frac{-A\sqrt{-\frac{3A^2wc_2^2-4k^2b_3p_1^2}{b_3}}\tanh\left(\frac{\zeta}{2}\sqrt{-\frac{3A^2wc_2^2-4k^2b_3p_1^2}{A^2b_3p_1^2}}\right)\sqrt{-\frac{3A^2wc_2^2-4k^2b_3p_1^2}{A^2b_3p_1^2}}b_3p_1+3A^2wc_2^2-4k^2a_3p_1^2}{\sqrt{-\frac{3A^2wc_2^2-4k^2b_3p_1^2}{b_3}}Ab_3c_2}. \tag{19}$$

Box I.

$$P(x,t)=\left(\frac{-A\sqrt{-\frac{3A^2wc_2^2-4k^2b_3p_1^2}{b_3}}\tanh\left(\frac{\zeta}{2}\sqrt{-\frac{3A^2wc_2^2-4k^2b_3p_1^2}{A^2b_3p_1^2}}\right)\sqrt{-\frac{3A^2wc_2^2-4k^2b_3p_1^2}{A^2b_3p_1^2}}b_3p_1+3A^2wc_2^2-4k^2a_3p_1^2}{\sqrt{-\frac{3A^2wc_2^2-4k^2b_3p_1^2}{b_3}}Ab_3c_2}\right)^{1/2}\times$$
$$e^{\iota(-kx_wt+\theta)}, \tag{20}$$

Box II.

Analytical soliton solutions

Using the proposed methodology, this section retrieves soliton solutions for the proposed model Eq. (10). Here, Eq. (7) has been solved implementing the unified approach to obtain soliton solutions.

In Eq. (7), balancing n'^2 and n^3 produces $N = 1$. The suggested solution has the form mentioned below:

$$W(\zeta)=\sum_{i=0}^{1}p_i\psi^i(\zeta),\quad r_1\neq 0, \tag{15}$$

with the auxiliary equation

$$(\psi'(\zeta))^{\epsilon}=\sum_{i=0}^{2\epsilon}c_i\psi^i(\zeta),\quad \epsilon=1,2. \tag{16}$$

Polynomial function solution

Solitary Wave Solution

For this purpose, put $\gamma = 1$ in the auxiliary Eq. (16), and so we obtain

$$W(\zeta)=p_0+p_1\psi(\zeta) \tag{17}$$
$$\psi'(\zeta)=c_0+c_1\psi(\zeta)+c_2\psi^2(\zeta).$$

By substituting Eq. (17) into Eq. (7), a system of non-linear equations is generated. This system will be handled further with the help of software such as Maple or Mathematica. The following outcomes are retrieved

$$b_2=\frac{-12\,A^2w\,c_2{}^2-Akb_4c_2\sqrt{-\frac{27\,A^2w\,c_2{}^2-36\,k^2b_3p_1{}^2}{b_3}}-16\,k^2b_3p_1{}^2}{Ac_2\sqrt{-\frac{27\,A^2w\,c_2{}^2-36\,k^2b_3p_1{}^2}{b_3}}},$$
$$p_0=\frac{-3(3\,A^2w\,c_2{}^2-4\,k^2b_3p_1{}^2)}{Ab_3c_2\sqrt{-\frac{27\,A^2w_rc_2{}^2-36\,k^2b_3p_1{}^2}{b_3}}},$$
$$b_1=-\frac{4b_3p_1{}^2}{3A^2c_2{}^2},\quad c_0=-2\,\frac{3\,A^2w\,c_2{}^2-4\,k^2b_3p_1{}^2}{c_2A^2b_3p_1{}^2},$$
$$b_1=\frac{1}{p_1A}\sqrt{-\frac{27\,A^2w\,b_2{}^2-36\,k^2b_3p_1{}^2}{b_3}}. \tag{18}$$

By solving the auxiliary equation $\psi'(\zeta) = c_0 + c_1\psi(\zeta) + c_2\psi^2(\zeta)$ and substituting together with (18), we find that in this case, Eq. (7) has the following solution which is given in Box I. Then we get the solution which is given in Box II. where $\zeta = x - vt$.

Soliton Wave Solution

Here for $\gamma = 2$, we obtain

$$W(\zeta)=p_0+p_1\psi(\zeta), \tag{21}$$
$$\psi'(\zeta)=\psi(\zeta)\sqrt{c_0+c_1\psi(\zeta)+c_2\psi^2(\zeta)}. \tag{22}$$

By putting Eq. (21) into Eq. (7), a non-linear equations system is formed. This system will be solved even more with the help of software such as Maple or Mathematica. The following parameters are identified:

$$a_2=-\frac{A^2b_1c_1-2\,kb_4p_1}{2p_1},\quad b_3=-3/4\,\frac{A^2b_1c_2}{p_1{}^2},\quad c_0=\frac{4(kb_1+w)}{A^2b_1},\quad p_0=0 \tag{23}$$

By solving the auxiliary equation $\psi'(\zeta) = \psi(\zeta)\sqrt{c_0 + c_1\psi(\zeta) + c_2\psi^2(\zeta)}$ and substituting together with (18), Eq. (4) has the solution as;

$$W(\zeta)=\left(48\,p_1\left(k^2a_1+\omega\right)B^2a_1e^{2\zeta\sqrt{\frac{k^2a_1+\omega}{B^2a_1}}}\right)\Big/\left(64\,e^{4\zeta\sqrt{\frac{k^2a_1+\omega}{B^2a_1}}}k^2a_1a_3p_1{}^2\right.$$
$$+64\,e^{4\zeta\sqrt{\frac{k^2a_1+\omega}{B^2a_1}}}\omega\,a_3p_1{}^2+$$
$$12\,e^{4\zeta\sqrt{\frac{k^2a_1+\omega}{B^2a_1}}}k^2a_4{}^2p_1{}^2-24\,e^{4\zeta\sqrt{\frac{k^2a_1+\omega}{B^2a_1}}}ka_2a_4p_1{}^2$$
$$+12\,e^{4\zeta\sqrt{\frac{k^2a_1+\omega}{B^2a_1}}}a_2{}^2p_1{}^2-$$
$$\left.12\,B^2e^{2\zeta\sqrt{\frac{k^2a_1+\omega}{B^2a_1}}}ka_1a_4p_1+12\,B^2e^{2\zeta\sqrt{\frac{k^2a_1+\omega}{B^2a_1}}}a_1a_2p_1+3\,B^4a_1{}^2\right), \tag{24}$$

then the obtained solution is

$$P(x,t)=$$
$$\left(\left(48\,p_1\left(k^2a_1+\omega\right)B^2a_1e^{2\zeta\sqrt{\frac{k^2a_1+\omega}{B^2a_1}}}\right)\Big/\left(64\,e^{4\zeta\sqrt{\frac{k^2a_1+\omega}{B^2a_1}}}k^2a_1a_3p_1{}^2\right.\right.$$
$$+64\,e^{4\zeta\sqrt{\frac{k^2a_1+\omega}{B^2a_1}}}\omega\,a_3p_1{}^2+ \tag{25}$$
$$12\,e^{4\zeta\sqrt{\frac{k^2a_1+\omega}{B^2a_1}}}k^2a_4{}^2p_1{}^2-24\,e^{4\zeta\sqrt{\frac{k^2a_1+\omega}{B^2a_1}}}ka_2a_4p_1{}^2$$
$$+12\,e^{4\zeta\sqrt{\frac{k^2a_1+\omega}{B^2a_1}}}a_2{}^2p_1{}^2-$$

$$12\,B^2 e^{2\zeta\sqrt{\frac{k^2a_1+\omega}{B^2a_1}}}\,k a_1 a_4 p_1$$
$$+\;12\,B^2 e^{2\zeta,\sqrt{\frac{k^2a_1+\omega}{B^2a_1}}}\,a_1a_2p_1+3\,B^4{a_1}^2\Big)\Big)^{1/2}e^{\iota(-kx_wt+\theta)}, \tag{26}$$

where $\zeta = x - vt$.

Rational function solution

To evaluate the rational solutions of the governing equation with the unified method, we assume that

$$W(\zeta)=\frac{\sum_{m=0}^{n} r_m\psi^m(\zeta)}{\sum_{m=0}^{j} s_m\psi^m(\zeta)},\quad n\geq j, \tag{27}$$

satisfying auxiliary equation,

$$(\psi'(\zeta))^{\gamma}=\sum_{i=0}^{\epsilon v} c_i\psi^i(\zeta),\quad \zeta=x-vt,\quad \gamma=1,2. \tag{28}$$

where r_m, s_m, and c_i are constants to be found. Utilizing Eq. (27) into equation into Eq. (7), system of algebraic equations in ψ is obtained. Now by utilizing some symbolic computing softwares like Maple or Mathematica, constants are obtained as follows

$$c_0=\frac{2(6\,k^2b_1{s_0}^2+3\,kb_4r_0s_0+6w\,{s_0}^2-3\,b_2r_0s_0-2\,b_3{r_0}^2)}{3(A^2b_1{s_1}^2)},$$
$$c_1=\frac{2(4\,k^2b_1s_0+kb_4r_0+4\,w\,s_0-b_2r_0)}{A^2b_1s_1},$$
$$c_2=4\frac{k^2b_1+w}{A^2b_1},\quad r_1=0. \tag{29}$$

Solving the auxiliary equation $\psi'(\zeta)=\sqrt{q_0+q_1\psi(\zeta)+q_2\psi^2(\zeta)}$, and substituting together the values in Eq. (29). The Eq. (4) has the following solution.

$$W(\zeta)=48\left(k^2b_1+w\right)s_1b_1A^2r_0\sqrt{\frac{k^2b_1+w}{A^2b_1}}e^{2\zeta\sqrt{\frac{k^2b_1+w}{A^2b_1}}}$$
$$\times\Bigg(-12\,A^2s_1\sqrt{\frac{k^2b_1+w}{A^2b_1}}r_0b_1\left(kb_4-b_2\right)e^{2\zeta\sqrt{\frac{k^2b_1+w}{A^2b_1}}}+$$
$$12\,A^2{s_1}^2b_1\left(k^2b_1+w\right)e^{4\zeta\sqrt{\frac{k^2b_1+w}{A^2b_1}}}$$
$$+16\,{r_0}^2\left(k^2b_1b_3+3/16\,k^2{b_4}^2-3/8\,kb_2b_4+w\,b_3+\frac{3\,{b_2}^2}{16}\right)\Bigg)^{-1}, \tag{30}$$

where by substituting Eq. (30) into equation Eq. (3), we get the solution of the governing equation

$$P(x,t)=\Bigg(48\left(k^2b_1+w\right)s_1b_1A^2r_0\sqrt{\frac{k^2b_1+w}{A^2b_1}}e^{2\zeta\sqrt{\frac{k^2b_1+w}{A^2b_1}}}$$
$$\times\Bigg(-12\,A^2s_1\sqrt{\frac{k^2b_1+w}{A^2b_1}}r_0b_1\left(kb_4-b_2\right)e^{2\zeta\sqrt{\frac{k^2b_1+w}{A^2b_1}}}$$
$$+12\,A^2{s_1}^2b_1\left(k^2b_1+w\right)e^{4\zeta\sqrt{\frac{k^2b_1+w}{A^2b_1}}}$$
$$+16\,{r_0}^2\Bigg(k^2b_1b_3+3/16\,k^2{b_4}^2-3/8\,kb_2b_4+$$
$$w\,b_3+\frac{3\,{b_2}^2}{16}\Bigg)\Bigg)^{-1}\Bigg)^{1/2}e^{\iota(-kx_wt+\theta)}, \tag{31}$$

where $\zeta = x - vt$.

Applications

In this part, we provide graphical illustrations of few of the determined results. It is important to mention here that explicit and consistent wave solutions are extracted by applying unified method. The Figs. 1–3 shows pictorial illustration of the obtained solutions in 3D and 2D depiction at some appropriate parameters. Fig. 1. dark soliton solution is the solitary solution in 3D and 2D. The graphical depiction of soliton polynomial solution is illustrated in Fig. 2 which is a bright soliton, whereas rational solutions are depicted in Fig. 3 which shows bright soliton.

In the next section, we will discuss our model via **bifurcation**.

Qualitative analysis of governing equation

The bifurcation of nonlinear of governing equation is investigated in the following section. To achieve our goal, we used the previously mentioned traveling wave solution to convert the model to an ordinary differential equation, Eq. (7).

By utilizing Eq. (7), the following planer dynamical system has been obtained

$$W'=z$$
$$z'=\frac{4(w+b_1k^2)W^2+b_1A^2z^2+4(kb_4-b_2)W^3-4b_3}{2b_1A^2W}. \tag{32}$$

However, the system in consideration is indeed not hamiltonian. Using Eq. (32), we retrieve

$$\frac{dz^2}{dW}=\frac{4(w+b_1k^2)W^2+b_1A^2z^2+4(kb_4-b_2)W^3-4b_3}{b_1A^2W}, \tag{33}$$

Since $W=0$ is the singular point of the Eq. (33), W can only have zero in exceptional conditions. Eq. (33) has solution

$$z^2=c_1W+\frac{2}{3b_1A^2}\left(6b_1k^2W^2-2b_3W^4+3b_4kW^3-3b_2W^2+12W^2\right), \tag{34}$$

we get

$$z^2-[c_1W+\frac{4b_3W^4}{3b_1A^2}+\frac{1}{3}\frac{6b_4k-6b_3}{b_1A^2}W^3+\frac{(12b_1k^2+12w)W^2}{b_1A^2}]=0, \tag{35}$$

where c_1 is the constant of integration. Consequently it is possible to obtain the equivalent conserved quantity.

$$H(W,z)$$
$$=z^2-\left[c_1W+\frac{4b_3W^4}{3b_1A^2}+\frac{1}{3}\frac{6b_4k-6b_3}{b_1A^2}W^3+\frac{(12b_1k^2+12w)W^2}{b_1A^2}\right], \tag{36}$$

that is conserved quantity. Since Eq. (36) is autonomous, the global phase portrait consists entirely of the system's contour lines. Now, using the entire discrimination system, we undertake a qualitative analysis based on the discussed model. Since we have Eq. (36) including its potential energy as

$$W=-\left[c_1W+\frac{4b_3W^4}{3b_1A^2}+\frac{1}{3}\frac{6b_4k-6b_3}{b_1A^2}W^3+\frac{(12b_1k^2+12w)W^2}{b_1A^2}\right], \tag{37}$$

moreover

$$W'=-\left[c_1+\frac{16b_3W^3}{3b_1A^2}+\frac{6b_3-6b_4k}{b_1A^2}W^2-2\frac{-(12b_1k^2+12w)W}{b_1A^2}\right],$$
$$W'=c_1-a_0W^3+a^1W^2+a_2W. \tag{38}$$

Let $J(W,z)$ be the linearized coefficient matrix at the equilibrium point (W,z). This matrix is termed as the system's **Jacobian** matrix. The determinant of the Jacobi matrix could be described as follows:

$$J(W,z)=\begin{vmatrix}0 & 1\\ -3a_0W^2+2a_1W+a_2 & 0\end{vmatrix}, \tag{39}$$

hence obtained Jacobian is

$$J(W,z)=3a_0W^2-2a_1W-a_2. \tag{40}$$

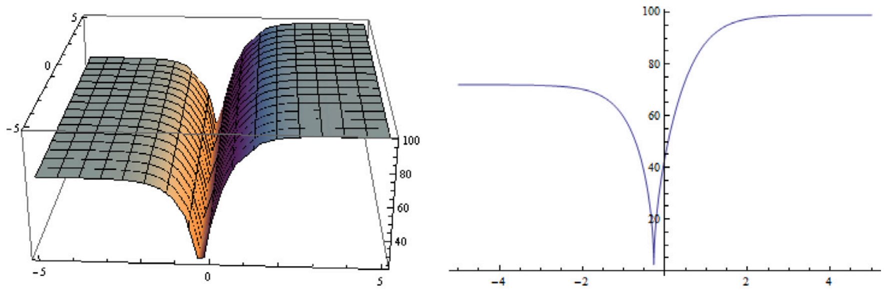

(a) 3D plot of Eq.(23) (b) 2D plot of Eq.(23)

Fig. 1. Dark soliton solution for the parametric values of $A = 0.75,\ w = -0.05,\ b_3 = 1,\ p_1 = 15,\ c_2 = -0.5,\ k = 0.4,\ \theta = 0.04,\ b_1 = 0.05$.

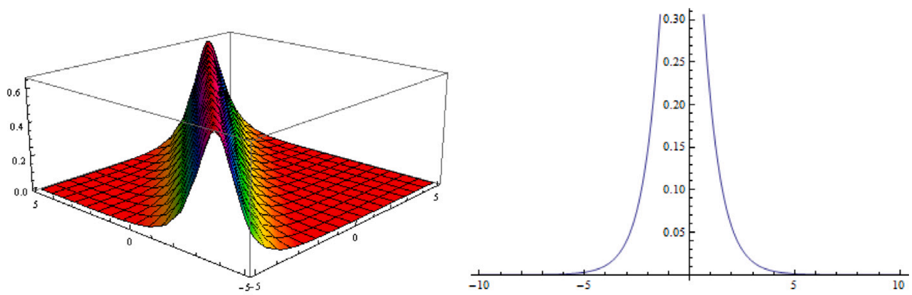

(a) 3D plot of Eq.(26) (b) 2D plot of Eq.(26)

Fig. 2. Bright soliton solution for the parametric values chosen as $A = 4,\ w = 2,\ b_3 = 2,\ p_1 = 0.5,\ c_2 = 1,\ k = -2,\ \theta = 0.05,\ b_4 = 0.5,\ b_1 = -0.25$.

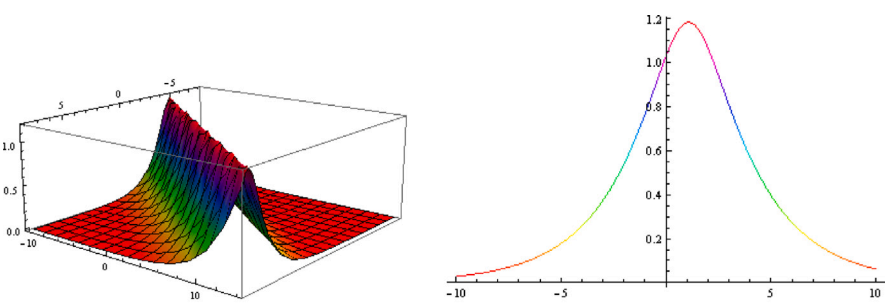

(a) 3D plot of Eq.(31) (b) 2D plot of Eq.(31)

Fig. 3. Bright soliton solution for the parametric values chosen as $A = 8,\ w = 0.05,\ b_3 = 2,\ b_2 = 4,\ c_2 = 1,\ k = -2,\ \theta = 0.02,\ b_4 = 0.5,\ b_1 = -0.015,\ r_0 = 0.2,\ s_1 = 0.2$.

The eigenvalues at a singular point $(f, 0)$ are simple to depict as follow

$$\lambda_{\pm}(W, 0) = \pm\sqrt{-(3a_0W^2 - 2a_1W - a_2)}. \tag{41}$$

Here $(W, 0)$ is saddle if $J(W, 0) < 0$, if $J(W, 0) > 0$, then its a center point, while cusp if $J(W, 0) = 0$.

Through presenting the discriminant for polynomial

$$\Delta = -27a_0^2c_1^2 - 18a_0a_1a_2c_1 + 4a_0a_2^3 - 4a_1^3c_1 + b_1^2b_2^2, \tag{42}$$

we get the following possibilities.

Case I: $\Delta = 0$ and $c_1 > 0,\ a_0 > 0,\ a_1 > 0,\ a_2 > 0$. Then

$$W' = (W - l)^2(W - s). \tag{43}$$

In this case, two equilibrium points $(l, 0)$ and $(s, 0)$ exist. Then by investigating the jacobian, the result is, $(l, 0)$ a cusp and $(s, 0)$ will be center. The phase portrait has been shown for $c_1 = 0.025$, $a_0 = 9.6225$ and $a_1 = 5$, $a_2 = 0.75$, we get $l = -0.0634$ and $s = 0.6464$.

Case II: $\Delta = 0$ and $c_1 < 0,\ a_0 < 0,\ a_1 > 0,\ a_2 > 0$. Then

$$W' = (W - l)^2(W - s). \tag{44}$$

Two equilibrium points $(l, 0)$ and $(s, 0)$ exist in this specific case. By examining jacobian the result shows that $(l, 0)$ a cusp and $(s, 0)$ will be saddle. The phase portrait has been shown for $c_1 = -1.025$, $a_0 = 0.375$ and $a_1 = 1.25$, $a_2 = 0.5$, we get $l = -2$ and $s = 0.6667$.

Case III: $\Delta = 0$ and $c_1 < 0,\ a_0 > 0,\ a_1 > 0,\ a_2 > 0$. Then

$$W' = (W - l)^2(W - s). \tag{45}$$

There seem to be two equilibrium points in this particular circumstance: $(l, 0)$ and $(s, 0)$. The result of studying the jacobian shows that $(l, 0)$ is a cusp and $(s, 0)$ is the center. For $c_1 = -0.25$, $a_0 = 3$, and $a_1 = 2$,

$a_2 = 0.25$, for these parametric values the equilibrium points are $l = 0.5$, and $s = -0.3333$, the phase portrait has been depicted.

Case IV: $\Delta = 0$ and $c_1 = 0$, $a_0 > 0$, $a_1 > 0$, $a_2 = 0$. Then

$$W' = (W - l)^2(W - s). \tag{46}$$

Two equilibrium points are there in this particular circumstance: $(l, 0)$ and $(s, 0)$. The result of studying the jacobian shows that $(l, 0)$ is a cusp and $(s, 0)$ is the center. For $c_1 = 0$, $a_0 = 0.035$, and $a_1 = 0.2$, $a_2 = 0$, the equilibrium points are $l = 0.5$, and $s = -0.3333$, the phase portrait for this case has been depicted.

Case V: $\Delta = 0$ and $c_1 = 0$, $a_0 > 0$, $a_1 > 0$, $a_2 = 0$. Then

$$W' = (W - l)^2(W - s). \tag{47}$$

Two equilibrium points are there in this particular circumstance: $(l, 0)$ and $(s, 0)$. The result of studying the jacobian shows that $(l, 0)$ is a cusp and $(s, 0)$ is the center. For $c_1 = 0$, $a_0 = 0.035$, and $a_1 = 0.2$, $a_2 = 0$, the equilibrium points are $l = 0.5$, and $s = -0.3333$, the phase portrait for this case has been depicted.

Case VI: $\Delta > 0$ and $c_1 > 0$, $a_0 > 0$, $a_1 > 0$, $a_2 > 0$. Then

$$W' = (W - l)(W - m)(W - n), \tag{48}$$

aforementioned equation has three equilibrium points $(l, 0)$, $(m, 0)$ and $(n, 0)$. In this region $(l, 0)$ and $(n, 0)$ are center, $(m, 0)$ is saddle. The phase portrait has been plotted for $c_1 = 0.5$, $a_0 = 2$, and $a_1 = 2$, $a_2 = 4$ where the equilibrium points are $l = -0.9049$, $m = -0.1354$, $n = 2.0403$

Case VII: $\Delta > 0$ and $c_1 = 0$, $a_0 > 0$, $a_1 > 0$, $a_2 > 0$. Then

$$W' = (W - l)(W - m)(W - n), \tag{49}$$

in the above equation we get three equilibrium points $(l, 0)$, $(m, 0)$ and $(n, 0)$. In this case $(l, 0)$ is center, $(m, 0)$ is saddle and $(n, 0)$ is also center. The phase portrait has been plotted for $c_1 = 0$, $a_0 = 1$, and $a_1 = 5$, $a_2 = 2$ where we get $l = -0.3723$, $m = 0$, and $n = 5.3723$.

Case VIII: $\Delta > 0$ and $c_1 > 0$, $a_0 = 0$, $a_1 > 0$, $a_2 > 0$. Then

$$W' = (W - l)(W - s). \tag{50}$$

Two equilibrium points are there in this particular circumstance: $(l, 0)$ and $(s, 0)$. By investigating jacobian shows that $(l, 0)$ is a center and $(s, 0)$ is the saddle. For $c_1 = 0.5$, $a_0 = 0$, and $a_1 = 1$, $a_2 = 2$, the equilibrium points are $l = -0.5$, and $s = -0.25$, the phase portrait for this case has been plotted.

Case IX: $\Delta > 0$ and $c_1 = 0$, $a_0 = 0$, $a_1 > 0$, $a_2 > 0$. Then

$$W' = (W - l)(W - s). \tag{51}$$

Two equilibrium points are there in this particular circumstance: $(l, 0)$ and $(s, 0)$. By investigating jacobian shows that $(l, 0)$ is a center and $(s, 0)$ is the saddle. For $c_1 = 0$, $a_0 = 0$, and $a_1 = 1$, $a_2 = 3$, the equilibrium points are $l = 3$, and $s = 0$, the phase portrait for this case has been plotted.

Case X: $\Delta < 0$. Then

$$W' = (W - s)[(W - l)^2 + m^2]. \tag{52}$$

Here $(s, 0)$ is only real equilibrium point and it is a saddle (see Figs. 4–12).

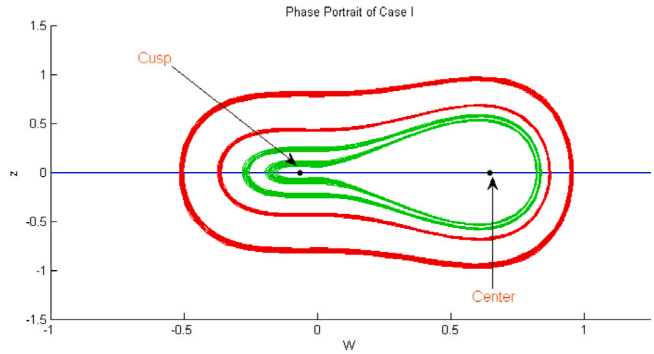

Fig. 4. Global phase portrait for **CaseI**.

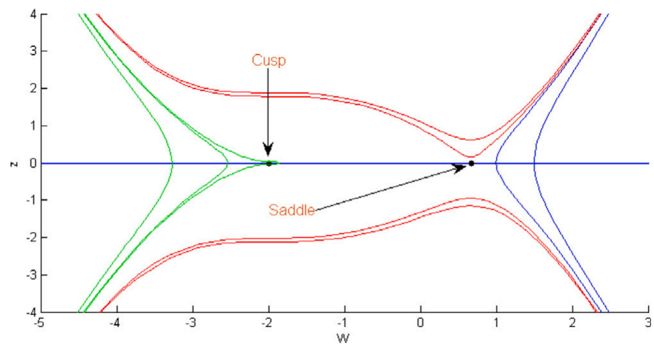

Fig. 5. Global phase portrait for **CaseII**.

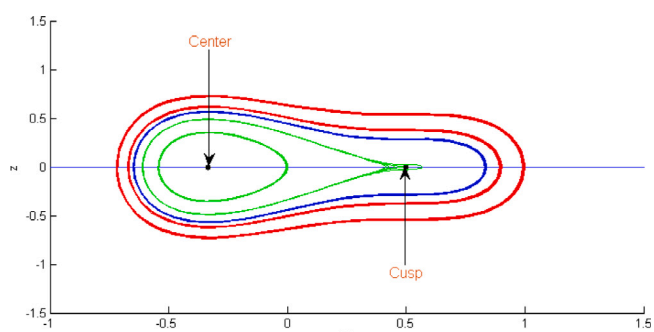

Fig. 6. Global phase portrait for **CaseIII**.

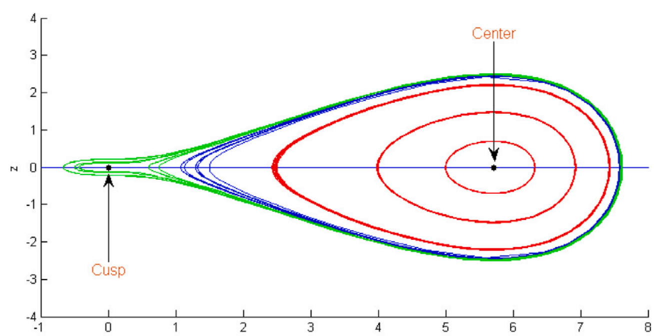

Fig. 7. Global phase portrait for **CaseIV**.

Conclusion

In this manuscript, the dynamics of optical solitons in the nonlinear Schrödinger equation (NLSE) with cubic–quintic law nonlinearity was studied. To extract new results, two strong methodologies was used. To extract the exact solution of governing equation, unified method was used. By employing this technique, the solutions were extracted in form of polynomial and rational form solutions. This technique provided us bright and dark solitons. Moreover, the solutions were graphically depicted showing that the obtained results made bright and dark

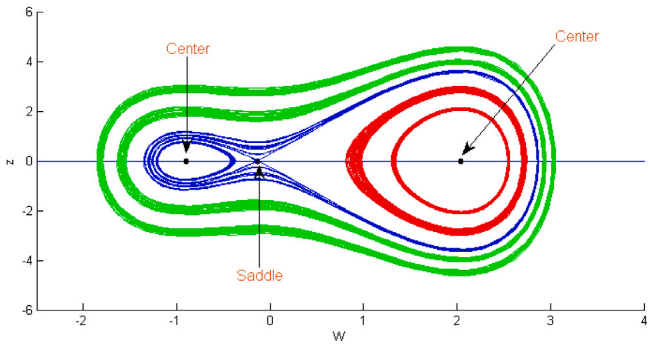

Fig. 8. Global phase portrait for **CaseV**.

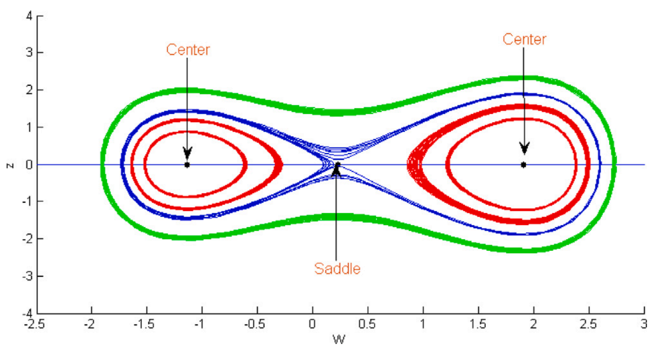

Fig. 9. Global phase portrait for **CaseVI**.

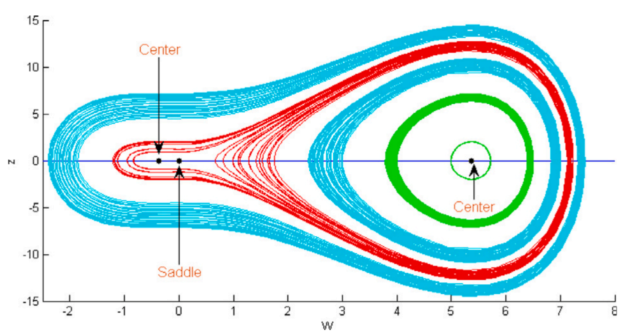

Fig. 10. Global phase portrait for **CaseVII**.

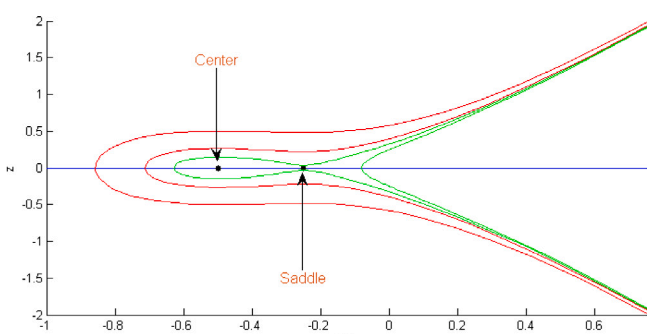

Fig. 11. Global phase portrait for **CaseVIII**.

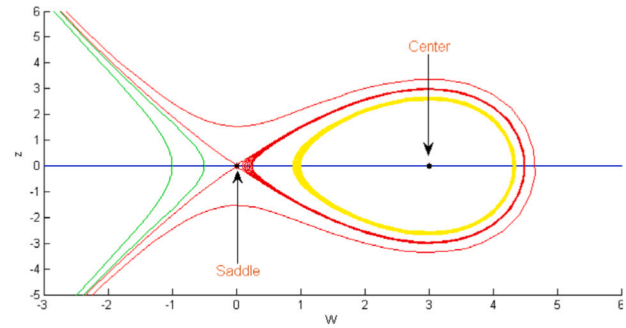

Fig. 12. Global phase portrait for **CaseIX**.

solitons. The equation was investigated through bifurcation for phase characterization. The system was transformed into a planer dynamical system, which was then transformed into a Hamiltonian system. The cases were then predicted and successfully depicted in phase portrait using the discriminant. The work contributes in the investigation of NLSE, showing that the applied techniques are simple, interesting and direct method to explore different NLSEs. The acquired solutions have been discovered to be novel and have never been presented before.

Declaration of competing interest

The authors declare that they have no known competing financial interests or personal relationships that could have appeared to influence the work reported in this paper.

Data availability

No data was used for the research described in the article.

Acknowledgment

Open Access funding provided by the Qatar National Library.

References

[1] Ma WX, Osman MS, Arshad S, Raza N, Srivasta HM. Practical analytical approaches for finding novel optical solitons in the single-mode fibers. Chin J Phys 2021;72:475–86.
[2] Huang G, Lv G, Fan Y, Geng C, Li X. Predictive optimization algorithm for beam combination systems based on adaptive fiber optics collimators. Opt Lasers Eng 2022;148:106753.
[3] Hosseini K, Mirzazedah M, Baleanu D, Salahshour S, Akinyemi L. Optical solitons of a high-order nonlinear schrodinger equation involving nonlinear dispersions and Kerr effect. Opt Quantum Electron 2020;54(177).
[4] Raza N, Zubair A. Bright, dark and dark-singular soliton solutions of nonlinear Schrödinger's equation with spatio-temporal dispersion. J Mod Opt 2018;65:1975–82.
[5] Raza N, Arshad S, Sial S. Optical-solitons for coupled Fokas-Lenells equation in birefringence fibres. Modern Phys Lett B 2019;33:1950317.
[6] Raza N, Javid A. Dynamics of optical solitons with Radhakrishnan-Kundu-Lakshamanan model via two reliable integration schemes. Optik 2019;178:557–66.
[7] Aguilar JFG, Osman MS, Raza N, Zubair A, Arshad S, Ghoneim ME, et al. Optical solitons in birefringent fibers with quadratic-cubic nonlinearity using three integration architectures. AIP Adv 2005;11(2):5, 0038038.
[8] Raza N, Arshad S, Javid A. Optical solitons and stability analysis for the generalized second-order nonlinear Schrodinger equation in an optical fibe. Int J Nonlinear Sci Numer Simul 2020;21(7–8):855–63.
[9] Eremenko S. Soliton nature' book preprint chapter 1. 2019, Translation wave of Scott Rossell.
[10] Gao W, Ismael HF, Husein AM, butt H. Optical soliton solutions of the cubic-quartic nonlinear Schrodinger and resonant nonlinear Schrodinger equation with the parabolic law. Appl Sci 2020;10(1):219.
[11] Hasegawa A, Tappert F. Transmission of stationary nonlinear optical pulses in dispersive dielectric fibers, I. Anomalous dispersion. Appl Phys Lett 1973;23(3).
[12] Mollenauer LF, Stolen JP, Gordan JP. Experimental observation of picosecond pulse narrowing and solitons in optical fibers. Phys Rev Lett 1980;45:1095.

[13] Wang M, Zhou Y, Li Z. Application of a homogeneous balance method to exact solutions of nonlinear equations in mathematical physics. Phys Lett A 1996;216:69–75.
[14] Moghaddam MY, Asgari A, Yazdani H. Exact travelling wave solutions for the generalized nonlinear Schrodinger (GNLS) equation with a source by extended tanh-coth, sine-cosine and exp-function methods. Appl Math Comp 2009;210:422–35.
[15] Taghizadeh N, Mirzazadeh M, Farahrooz F. Exact solutions of the nonlinear Schrodinger equation by the first integral method. J Math Anal Appl 2011;374:549–53.
[16] Arshad M, Seadaway AR, Lu D. Elliptic function and solitary wave solutions of the higher-order nonlinear Schrodinger dynamical equation with fourth-order dispersion and cubic-quintic nonlinearity and its stability. Eur Phys J Plus 2017;132:371.
[17] Rizvi STR, Ali K, Ahmed M. Optical solitons for Biswas-Milovic equation by new extended auxiliary equation method. Optik 2020;204:164181.
[18] Arshad S, Arshad L. Optical soliton solutions for nonlinear Schrodinger equation. Optik 2019;195:163077.
[19] Cao R, Zhang J. Trial function method and exact solutions to the generalized nonlinear Schrödinger equation with time-dependent coefficient. Chin Phys B 2013;22:100507.
[20] Khater MMA, Jhangeer A, Razazadeh H, Akinyemi L, Akbar MA, Inc M. Propagation of new dynamics of longitudinal bud equation among a magneto-electro-elastic round rod. Modern Phys Lett B 2021;35:2150381.
[21] Mirzazadeh M, Akinyemi L. A novel integration approach to study the perturbed Biswas-Milovic equation with Kudryashov's law of refractive index. Optik 2022;252:168529.
[22] Abbagari S, Boutou TB. Modulated wave and modulation instability gain brought by the cross-phase modulation in birefringent fibers having anti-cubic nonlinearity. Phys Lett A 2022;442:128191.
[23] Yao SW, Senol M. Dynamics of optical solitons in higher-order Sasa–Satsuma equation. Results Phys 2021;30:104825.
[24] Nisar KS, Akinyemi L. New solutions for the generalized resonant nonlinear Schrödinger equation. Results Phys 2022;33:105153.
[25] Nisar KS, Rezazadah H. New perturbed conformable Boussinesq-like equation: Soliton and other solutions. Results Phys 2022;33:105200.
[26] Mahak N, Akram G. Extension of rational sine-cosine and rational sinh-cosh techniques to extract solutions for the perturbed NLSE with Kerr law nonlinearity. Eur Phys J Plus 2019;134(159).
[27] Ali A, Seadway AR, Lu D. Schrodinger equation with the dual power law nonlinearity and resonant nonlinear Schrodinger equation and their modulation instability analysis. Optik 2017;145:79–88.
[28] Xu LP, Zang LP. Exact solutions to two higher order nonlinear Schrodinger equations. Chaos Solit Fractals 2007;31(4):937–42.
[29] Shehata MSM. A new solitary wave solution of the perturbed nonlinear Schrodinger equation using a Riccati-Bernoulli sub-ODE method. Phys Sci Int J 2016;11(6):80–4.
[30] Hassan SZ, Abdulrehman MAE. A Riccati-Bernoulli sub-ODE method for some nonlinear evolution equations. Int J Nonlinear Sci Numer Simul 2019;20(3–4):303–13.
[31] Raza N, Seadway AR, Kaplan M, Butt AR. Symbolic computation and sensitivity analysis of nonlinear Kudryashov's dynamical equation with applications. Phys Scr 2021;96(10):105216.
[32] Hernandez SM, Bonetti J, Linale N, Grosz DF, Fierens PI. Soliton solutions and self-steepening in the photon-conserving nonlinear Schrodinger equation. Waves Random Complex Media 2020;1856970.
[33] Arshad S, Raza N. Optical solitons perturbation of Fokas-Lenells equation with full nonlinearity and dual dispersion. Chin J Phys 2020;63:314–24.
[34] Raza N, seadway AR, Jhangeer A, Butt AR, Arshad S. Dynamical behavior of micro-structured solids with conformable time fractional strain wave equation. Phys Lett A 2020;384(27):126683.
[35] Javid A, Raza N. Chiral solitons of the (1+2)-dimensional nonlinear Schrodinger's equation. Modern Phys Lett B 2019;33(32):1950401.
[36] Rasheed NM, Al-Amr MO, Az-Zo'bi EA. Stable optical solitons for the higher-order non-Kerr NLSE via the modified simple equation method. Mathematics 2021;9(16):9161986.
[37] Bulut H, Pandir Y, Demiray ST. Exact solutions of nonlinear Schrodinger's equation with dual power-law nonlinearity by extended trial equation method. Wave Random Complex Media 2014;24(4):939246.
[38] Ekici M, Mirzazadeh M, Sonmezoglu A, Ullah MZaka, Zhou Q, Triki H, et al. Optical solitons with anti-cubic nonlinearity by extended trial equation method. Optik 2017;136:368–73.
[39] Vyas VM, Patel P, Panigrahi PK, Kumar CN, Greiner W. Chirped chiral solitons in the nonlinear Schrödinger equation with self-steepening and self-frequency shift. Phys Rev A 2008;78:021803.
[40] Kumar Ha, Chand F. Dark and bright solitary wave solutions of the higher order nonlinear Schrödinger equation with self-steepening and self-frequency shift effects. J Nonlinear Opt Phys Mater 2013;22(01).
[41] Alka Goyal A, Gupta R, Kumar CN, Raju TS. Chirped femtosecond solitons and double-kink solitons in the cubic-quintic nonlinear Schrödinger equation with self-steepening and self-frequency shift. Phys Rev A 2011;(84):063830.
[42] Raza N, Rafiq MH, Kaplan M, Kumar S, Chu YM. The unified method for abundant soliton solutions of local time fractional nonlinear evolution equations. Results Phys 2021;22:103979.
[43] Javid A, Raza N, Osman MS. Multi-solitons of thermophoretic motion equation depicting the wrinkle propagation in substrate-supported graphene sheets. Commun Theor Phys 2019;71(4):362.
[44] Raza N, Jhangeer A, Arshad S, Butt AR, Chu Y. Dynamical analysis and phase portraits of two-mode waves in different media. Chaos 2020;19:103650.
[45] Saha A. Bifurcation, periodic and chaotic motions of the modified equal width-Burgers (MEW-Burgers) equation with external periodic perturbation. Nonlinear Dynam 2017;87:2193–201.
[46] Elmandouha AA, Ibrahim AG. Bifurcation and travelling wave solutions for a (2+1)-dimensional KdV equation. J King Saud Univ Sci 2020;14(2020):139–47.